Human Genetics (2019) 138:21–35
https://doi.org/10.1007/s00439-018-1951-7

ORIGINAL INVESTIGATION

Delineation of *LZTR1* mutation-positive patients with Noonan syndrome and identification of LZTR1 binding to RAF1–PPP1CB complexes

Ikumi Umeki[1] · Tetsuya Niihori[1] · Taiki Abe[1] · Shin-ichiro Kanno[2] · Nobuhiko Okamoto[3] · Seiji Mizuno[4] · Kenji Kurosawa[5] · Keisuke Nagasaki[6] · Makoto Yoshida[7] · Hirofumi Ohashi[8] · Shin-ichi Inoue[1] · Yoichi Matsubara[9] · Ikuma Fujiwara[10] · Shigeo Kure[11] · Yoko Aoki[1]

Received: 20 July 2018 / Accepted: 21 October 2018 / Published online: 27 October 2018

Abstract

RASopathies are a group of developmental disorders caused by mutations in genes that regulate the RAS/MAPK pathway and include Noonan syndrome (NS), Costello syndrome, cardiofaciocutaneous syndrome and other related disorders. Whole exome sequencing studies recently identified *LZTR1, PPP1CB* and *MRAS* as new causative genes in RASopathies. However, information on the phenotypes of *LZTR1* mutation-positive patients and functional properties of the mutations are limited. To identify variants of *LZTR1, PPP1CB*, and *MRAS*, we performed a targeted next-generation sequencing and reexamined previously analyzed exome data in 166 patients with suspected RASopathies. We identified eight *LZTR1* variants, including a de novo variant, in seven probands who were suspicious for NS and one known de novo *PPP1CB* variant in a patient with NS. One of the seven probands had two compound heterozygous *LZTR1* variants, suggesting autosomal recessive inheritance. All probands with *LZTR1* variants had cardiac defects, including hypertrophic cardiomyopathy and atrial septal defect. Five of the seven probands had short stature or intellectual disabilities. Immunoprecipitation of endogenous LZTR1 followed by western blotting showed that LZTR1 bound to the RAF1–PPP1CB complex. Cells transfected with a small interfering RNA against *LZTR1* exhibited decreased levels of RAF1 phosphorylated at Ser259. These are the first results to demonstrate LZTR1 in association with the RAF1–PPP1CB complex as a component of the RAS/MAPK pathway.

Introduction

RASopathies are a family of syndromes caused by mutations in genes encoding various components of the RAS/MAPK pathway, which regulates cellular proliferation, differentiation,

Electronic supplementary material The online version of this article (https://doi.org/10.1007/s00439-018-1951-7) contains supplementary material, which is available to authorized users.

✉ Yoko Aoki
aokiy@med.tohoku.ac.jp

[1] Department of Medical Genetics, Tohoku University School of Medicine, 1-1 Seiryomachi, Aobaku, Sendai 980-8574, Japan

[2] Division of Dynamic Proteome in Cancer and Aging, Institute of Development, Aging and Cancer, Tohoku University, Sendai, Japan

[3] Department of Medical Genetics, Osaka Women's and Children's Hospital, Izumi, Japan

[4] Department of Pediatrics, Central Hospital, Aichi Human Service Center, Kasugai, Japan

[5] Division of Medical Genetics, Kanagawa Children's Medical Center, Yokohama, Japan

[6] Division of Pediatrics, Department of Homeostatic Regulation and Development, Niigata University Graduate School of Medical and Dental Sciences, Niigata, Japan

[7] Department of Pediatrics, Sano Kosei General Hospital, Sano, Japan

[8] Division of Medical Genetics, Saitama Children's Medical Center, Saitama, Japan

[9] National Research Institute for Child Health and Development, Tokyo, Japan

[10] Department of Pediatric Endocrinology and Environmental Medicine, Tohoku University Graduate School of Medicine, Sendai, Japan

[11] Department of Pediatrics, Tohoku University School of Medicine, Sendai, Japan

and cell death (Zhang and Dong 2007). Of these, Noonan syndrome (NS; MIM 163950), Costello syndrome (MIM 218040), and cardiofaciocutaneous (CFC) syndrome (MIM 115150) are characterized by a distinctive facial appearance, congenital heart disease, skeletal anomaly, and intellectual disability (Aoki et al. 2008). It is critical to distinguish among these syndromes because they differ in their incidence rates with respect to developmental delay and cancer risk (Nava et al. 2007; Villani et al. 2017). Distinguishing these syndromes based on the clinical manifestations alone is challenging; hence, molecular diagnosis should also be considered.

Recent advances in next-generation sequencing (NGS) enabled whole exome sequencing (WES) of genes in patients with RASopathies, leading to the identification of new causative genes. *RIT1* was the first causative gene of NS identified by WES (Aoki et al. 2013). Thereafter, *A2ML1* (Vissers et al. 2015), *RASA2, SPRY1* (Chen et al. 2014), *SOS2, LZTR1* (Yamamoto et al. 2015), *PPP1CB* (Gripp et al. 2016), and *MRAS* (Higgins et al. 2017) were demonstrated to be associated with RASopathies using WES. However, not much is known about the specific contributions of these recently identified genes to the development of NS.

LZTR1 is a tumor suppressor gene that encodes a protein belonging to the BTB-Kelch superfamily. LZTR1 (leucine zipper-like transcription regulator 1) is a Golgi-resident protein involved in apoptosis (Nacak et al. 2006) and ubiquitination, similarly to other BTB proteins (Lu and Pfeffer 2014; Stogios and Prive 2004). However, the exact function of LZTR1, particularly, whether it participates in the RAS/MAPK signal pathway, remains unknown. PPP1CB (protein phosphatase 1 catalytic subunit beta) constitutes the catalytic subunit of protein phosphatase 1 (PP1). PP1 was previously reported to form a complex with SHOC2 (leucine-rich repeat protein SHOC-2), coded by a causative gene of Noonan-like syndrome, and activate ERK by dephosphorylating RAF (Rodriguez-Viciana et al. 2006; Young et al. 2013).

The aim of this study was to elucidate the frequencies of mutations in the more recently identified genes *LZTR1, PPP1CB*, and *MRAS* in patients with RASopathies. For this purpose, we designed an NGS panel and conducted a comprehensive gene analysis of individuals with RASopathies or with clinically overlapping features, who were unidentified for pathogenic mutation. In addition, we searched for potential binding proteins of LZTR1 using immunoprecipitation analysis to clarify its involvement in the RAS/MAPK signaling pathway.

Results

Targeted NGS and WES

In the targeted NGS panel, we assayed 41 genes responsible for RASopathies or genetic syndromes with congenital anomalies (Supplementary Table 1). The targeted regions were designed to include coding exons with 50-bp intronic flanking bases and 3′ and 5′ untranslated regions (UTRs) using the SureDesign system (Agilent Technologies, Santa Clara, CA, USA). The regional source information of coding exons was extracted from the RefSeq, Ensembl, CCDS, Gencode, VEGA, SNP, or CytoBand databases. Of the total targeted region of 369,481 bp, 363,408 bp (98.36% coverage) was expected to be covered by 6092 reads.

We performed targeted NGS analysis in 142 patients with suspected RASopathies or related clinical phenotypes without any mutations in the exons of major RASopathy genes. Using the targeted panel, a total of 7384 variants were detected. Among these, four variants of *LZTR1* were detected in three patients and none showed any variants of *MRAS*. One of the *LZTR1* variants, c.742G>A, p.(G248R), was a previously reported pathogenic variant. Furthermore, we reexamined the exome data of 24 patients with RASopathies and identified four rare variants in *LZTR1* in four additional patients, and one variant in *PPP1CB* in another patient. No variant of *MRAS* was detected. In total, eight variants of *LZTR1* were identified in seven patients in the current study (Table 1). All missense variants detected in the current study were predicted damaging in silico. Since there were several patients with *LZTR1* variants, we next determined the associated clinical symptoms and the functions of these variants.

Clinical manifestations in patients with *LZTR1* variants and their families

Eight *LZTR1* variants were identified in seven patients. All patients were clinically suspected to have NS because they shared NS-related clinical manifestations, including relative macrocephaly, NS-related facial appearance, heart defects, intellectual disability, or short stature. Two of the patients (NS269 and NS876) did not exhibit any of the typical facial features. The clinical manifestations of patients with the *LZTR1* variants are listed in Table 2. The age of patients ranged from 2 to 16 years of age at assessment, and the average age was 9.6 years. The initial diagnoses of the patients were NS or suspected NS. All patients with the *LZTR1* variants had cardiac defects. The most common heart disease in the current study cohort was hypertrophic cardiomyopathy. Intellectual disability and short stature (71.4% and 71.4%, respectively) were frequent in the current study.

Echocardiography performed on patient NS269 (Fig. 1a–c), a boy born at 40 weeks' gestation with a birth weight of 2712 g, revealed pulmonary stenosis (PS). The patient NS269 showed developmental delay from infancy and presented with febrile convulsion at 5 years of age and with epilepsy at 7 years of age. He developed short stature, hyperacusis, scoliosis, and severe intellectual disability at

Table 1 Variants in *LZTR1* and *PPP1CB* detected in this study

Gene	RefSeq No.	Mutation type	Nucleotide change	Protein change	Zygosity	HGMD	1000 Genomes	dbSNP137	HGVD	iJGVD	SHIFT	PolyPhen2	Mutation Taster
LZTR1	NM_006767	Missense	c.428A>G	p.N143S	Heterozygous	NR	NR	NR	NR	NR	D	D	Disease causing
LZTR1	NM_006767	Frameshift	c.604_605del	p.M202fs	Heterozygous	NR	NR	NR	NR	NR	NA	NA	Disease causing
LZTR1	NM_006767	Missense	c.742G>A	p.G248R	Heterozygous	Noonan syndrome	NR	rs869320686	NR	NR	D	D	Disease causing
LZTR1	NM_006767	Deletion	c.756_758del	p.N253del	Heterozygous	NR	NR	NR	NR	NR	NA	NA	Disease causing
LZTR1	NM_006767	Missense	c.848G>A	p.R283Q	Heterozygous	NR	NR	NR	NR	NR	D	D	Disease causing
LZTR1	NM_006767	Missense	c.1660G>C	p.A554P	Heterozygous	NR	NR	NR	NR	NR	D	D	Disease causing
LZTR1	NM_006767	Splicing	c.2069+2T>C		Heterozygous	NR	NR	NR	NR	NR	NA	NA	NA
LZTR1	NM_006767	Missense	c.2102C>A	p.P701H	Heterozygous	NR	NR	NR	NR	NR	D	D	Disease causing
PPP1CB	NM_206876	Missense	c.146C>G	p.P49R	Heterozygous	Noonan-like syndrome with loose anagen hair	NR	rs886037952	NR	NR	D	D	Disease causing

HGMD Human Gene Mutation Database, *1000 Genomes* 1000 Genomes Project phase 3, *HGVD* Human Genetic Variation Database, *iJGVD* integrative Japanese, *NR* not reported, *NA* not applicable, *D(SHIFT)* damaging, *T* tolerated, *D(Polyphen2)* probably damaging, *P* possibly damaging, *B* benign

10 years of age. Analysis of his parental DNA revealed that the variation c.848G>A, p.(R283Q) in the patient NS269 had occurred de novo. He also demonstrated microcephalus and dysmorphic features, including thick eyebrow, low-set ears, long philtrum, and highly arched palate. At 11 years of age, his height was 120 cm (− 3.4 SD), body weight was 18.3 kg (− 2.4 SD), and head circumference was 49.5 cm (− 2.6 SD). In the patient NS876, an increase in nuchal translucency was detected at 10 weeks' gestation using fetal ultrasonography. Chorionic villus sampling was performed at 13 weeks' gestation, and the fetal karyotype was normal (46, XY). He was born at 40 weeks' gestation by vacuum extraction, and his birth weight was 3400 g. He showed a concealed penis but not cryptorchidism. Cardiac murmur was detected at 15 days of age. An echocardiogram revealed peripheral PS and anomalous origin of the coronary artery. He had mild hypertelorism, downslanting palpebral fissures, and lower eyelid retraction. Because of his NS-like facial appearance and heart defects, the patient was suspected to have NS. A *LZTR1* variant (c.742G>A, p.(G248R)) that has been reported in an autosomal dominant (AD) family (Yamamoto et al. 2015) was detected in the patient NS876 as well as in his mother. She had ventricular septal defect, which was closed spontaneously during the early childhood. She had mild hypertelorism and downslanting palpebral fissures that were less severe than the proband. The two missense variants (p.(R283Q) and p.(G248R)) were concluded as likely pathogenic because of de novo occurrence (p.(R283Q)), inheritance in two families in an AD trait (p.(G248R)), identification in glioblastoma (p.(G248R)) or bile duct tumor [(p.(R283Q)) by Catalogue of Somatic Mutations in Cancer database], and failure of detection in SNP databases, including ExAC, 1000 genome, HGVD or iJGVD.

The patient NS659 was referred to a physician for intense scrutiny of her short stature at 10 years of age. She had distinctive facial features suggestive of NS, hypertrophic cardiomyopathy (HCM), pectus excavatum, and 5th brachymetapody. She had shown mild intellectual disability until graduation from the elementary school and mental development is subsequently improved. The patient had two *LZTR1* variants: c.2069+2T>C and c.2102C>A, p.(P701H) that were inherited from her father and mother, respectively. The father and mother did not have short stature, NS-like facial appearance, or congenital heart disease. We confirmed that c.2069+2T>C causes exon 17 skipping (Supplementary Fig. 1), suggesting that truncated protein would be produced by mRNA without the sequences in exon17. c.2102C>A, p.(P701H) is located in the BTB2 domain, where autosomal recessive (AR) NS-related variants have been identified. These results suggest that the proband has AR NS detected in trans with a variant.

Table 2 Clinical manifestations of the patients with LZTR1 variations

	NS269	NS876	NS659	NS808	NS562	NS535	NS130
Mutation	c.848G>A, p.R283Q	c.742G>A, p.G248R	c.2102C>A, p.P701H c.2069+2T>C	c.428A>G, p.N143S	c.604_605del, p.M202fs	c.756_758del, p.N253del	c.1660G>C, p.A554P
Sex	M	M	F	M	F	M	F
Age	11 years	2 years	14 years	8 years	5 years	11 years	16 years
Initial diagnosis	Noonan syndrome	Noonan-like syndrome	Noonan syndrome	Noonan syndrome	Noonan syndrome	Noonan syndrome	Noonan syndrome
Gestational age	40 weeks	40 weeks	38 weeks	36 weeks	36 weeks	NA	NA
Birth weight	2712 g	3400 g	2888 g	3602 g	2474 g	NA	NA
Nuchal translucency	NA	+	−	NA	−	NA	NA
Fetal hydrops	−	−	−	−	Pleural effusion	NA	NA
Relative macrocephaly	−	−	−	+	+	+	+
Hypertelorism	−	+	+	+	+	+	+
Downslanting palpebral fissures	+	−	−	NA	−	+	+
Ptosis	−	+	−	NA	+	+	+
Epicanthal folds	+	−	−	+	+	+	+
Low-set ears	+	+	+	+	+	+	+
Sparse eyebrows	+	−	+	+	+	−	+
Bitemporal constriction	+	−	−	+	+	−	+
High cranial vault	+	−	−	+	+	−	+
Hypoplasia of supraorbital ridges	+	−	−	+	+	+	+
Cleft palate	−	−	−	−	−	−	−
Highly arched palate	+	+	−	−	+	NA	−
Short stature	+ −3.4SD	−	+ −2.1SD	+	+ −3.1SD	+	−
Short neck	+	−	+	−	+	+	+
Webbing of neck	+	−	−	−	+	+	+
Cubitus valgus	−	−	−	−	−	+	+
Scoliosis	+	−	+	−	−	−	−
Pectus excavatum	−	−	+	−	−	−	−
Pectus carinatum	−	−	−	+	−	+	−
Curly hair	−	−	−	−	−	+	+
Hyperelastic skin	+	−	−	−	−	−	+
Eczema	−	−	−	−	−	−	−
Hyperkeratosis	+	−	−	+	−	+	+
Wrinkled palms and soles	+	−	−	+	−	+	+
Hyperpigmentation	+	−	+	+	−	+	+
Café au lait spots	+	−	−	−	−	−	−
Naevus	−	−	−	+	−	−	+
Cardiac defects	+	+	+	+	+	+	+

Table 2 (continued)

	NS269	NS876	NS659	NS808	NS562	NS535	NS130
HCM	−	−	+	+	+	+	+
ASD	+	−	−	−	+	−	+
VSD	+	−	−	−	−	−	−
PS	+	−	−	−	+	−	−
Arrhythmia	−	−	−	−	+	−	−
Other	PDA	Anomalous origin of coronary artery	−	NA	−	−	−
Renal abnormality	NA	NA	−	−	−	NA	−
Cryptorchidism	−	−	N/A	+	N/A	−	N/A
Coagulation defects	−	NA	NA	−	−	−	NA
Intellectual disability	IQ36	−	Mild	+	DQ94	Mild	+
Convulsion	NA	−	−	−	−	NA	−
Feeding disorder	NA	−	−	−	−	NA	−
Miscellaneous	−	Concealed penis	Squint, amblyopia 5th brachymetapody	Puffy palms	−	Visual field contraction Optic atrophy	−
Father	WT	WT	c.2069+2T>C/WT	p.N143S/WT	p.M202fs/WT	NA	p.A554P/WT
Mother	WT	p.G248R/WT	p.P701H/WT	WT	WT	NA	WT

M male, *F* female, *HCM* hypertrophic cardiomyopathy, *ASD* atrial septal defect, *VSD* ventricular septal defect, *PS* pulmonary stenosis, *PDA* patent ductus arteriosus, *NA* not available, *N/A* not applicable, *WT* wild type

Patient NS808 (Fig. 1d–f) is a boy with short stature, relative macrocephaly, mild developmental delay, hypersensitivity, thick palms (Fig. 1f), mild dark skin, a naevus, and HCM. A missense variant in *LZTR1*, c.428A>G, p.(N143S), was identified in the patient NS808 and his father, who did not show any facial dysmorphology, heart defects, or intellectual disability. In the patient NS562 (Fig. 1g), fetal ultrasonography had revealed pleural effusion, amniotic fluid excess, and heart defect. She was born at 36 weeks' gestational age with a birth weight of 2474 g. At 2 months of age, she showed typical facial features of NS, including hypertelorism, ptosis, epicanthal fold, low-set ears, sparse eyebrows, hypoplasia of supraorbital ridge, highly arched palate, bitemporal constriction, and relative macrocephaly. Atrial septal defect (ASD) and non-occlusive HCM were detected by echocardiography. Her height was 99 cm (− 3.3 SD), weight was 13.8 kg (− 2.2 SD), and head circumference was 49.1 cm (− 1.3 SD) at 6 years of age. She showed a mild developmental delay. A *LZTR1* variant, c.604_605del, p.(M202fs), was identified in the proband. The same variant was identified in the father with no clinical features of NS. His height was normal for a Japanese adult. The patient NS535 had distinctive facial features of NS, short stature, webbing neck, cubitus valgus, pectus carinatum, hyperkeratosis, and developmental delay. An inframe deletion, c.756_758del, p.(N253del), was identified in the proband. Her mother and elder brother were also diagnosed as having NS. However, their samples could not be obtained because they shifted to another hospital. The patient NS130 (Fig. 1h, i) showed a distinctive craniofacial appearance, including relative macrocephaly, hypertelorism, downslanting palpebral fissures, and low-set ears. In addition, she had HCM, ASD, and intellectual disability. She was suspected as having Costello syndrome at the age of 4 years; however, no *HRAS* variant was identified using Sanger sequencing. Her clinical diagnosis has changed to NS with age. In the current study, c.1660G>C, p.(A554P) in *LZTR1* was identified in her as well as her father, who does not have short stature, intellectual disability, or NS-related facial features. These four variants—p.(N143S), p.(M202fs), p.(N253del), and p.(A554P)—were not identified in the SNP databases, including ExAC, 1000genome, HGVD or iJGVD. In silico analysis for p.(N143S) and p.(A554P) were predicted as damaging. Any clinical manifestations, including distinctive facial appearance, heart defects, or intellectual disability were not observed in a parent. In summary, the pathogenicity of four identified variants, including c.428A>G, p.(N143S); c.604_605del, p.(M202fs); c.1660G>C, p.(A554P); and

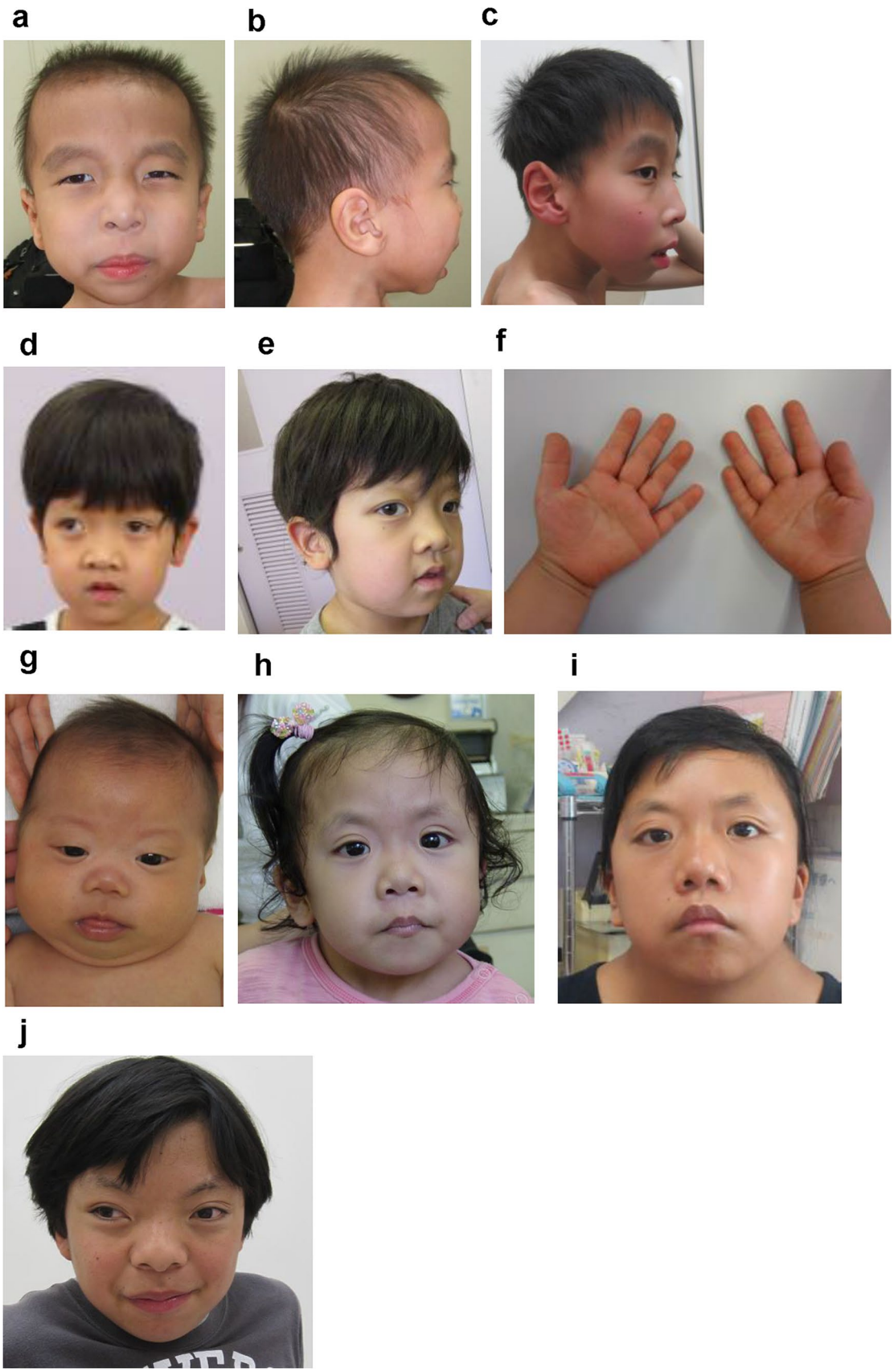
a
b
c
d
e
f
g
h
i
j

◂**Fig. 1** Photographs of four patients with *LZTR1* variants. NS269 at 4 years of age (**a, b**) or 10 years of age (**c**). **d–f** NS808 at 5 years of age. **g** NS562 at 2 months. NS 130 at 5 years (**h**) or 16 years of age (**i**). **j** A patient with PPP1CB variant at 16 years of age

c.756_758del, p.(253del), remains inconclusive. These four variants may be associated with AD NS with incomplete penetrance. Alternatively, these variants could cause AR NS, whereas another variant remains unidentified.

PPP1CB variants

We found a known *PPP1CB* variant in one patient (Table 1), and no other rare variants were detected in this gene. The *PPP1CB* variant was not present in either of the parents. The clinical manifestations of the patient are presented in Table 4 and Fig. 1j. The patient fulfilled the diagnostic criteria; however, he did not have any hair-associated symptoms, including sparse, slow growing hair, which are considered as a typical feature of patients with *PPP1CB* variants. Surgical repair for ASD and PS was performed when the patient was 5 months old. Undescended testis was also treated. He showed dysmorphic features of NS, including hypertelorism, upslanting palpebral fissures, epicanthal fold, low-set ears, sparse eyebrows, hypoplasia of supraorbital ridge, strabismus, bulbous nose, highly arched palate, and webbed neck.

LZTR1-binding proteins

Whether LZTR1 is involved in the RAS/MAPK signaling remains unclear; therefore, we investigated whether LZTR1 bound to proteins comprising the RAS/MAPK signal transduction pathway. First, we performed immunoprecipitation with an anti-LZTR1 antibody in HEK293 cell extracts, and the immune complexes were analyzed by liquid chromatography–tandem mass spectrometry. As a result, we identified PPP1CB in the immune complex containing endogenous LZTR1 (data not shown). Based on recent reports suggesting PPP1CB as a component of the RAF1/SHOC2 complex, we examined the interaction between LZTR1 and the RAF1/SHOC2/PPP1CB complex by western blot analysis of the immunoprecipitated samples using antibodies against RAF1, SHOC2, PPP1CB, and PTPN11. Endogenous LZTR1 could bind to RAF1, SHOC2, and PPP1CB but not to PTPN11 (Fig. 2a). We next performed a co-immunoprecipitation using the extracts of HEK293 cells coexpressing LZTR1-FLAG/RAF1-MYC or LZTR1-FLAG/PPP1CB-V5. Co-immunoprecipitation using the FLAG-M2 agarose for LZTR1 revealed the presence of MYC-tagged RAF1 and V5-tagged PPP1CB in the immune complexes containing the LZTR1-FLAG (Fig. 2b, c, respectively).

To investigate the impact of *LZTR1* variants on RAS/MAPK signal transduction, we performed a reporter assay using two *LZTR1* variants. The p.(G248R), which was identified in the patient NS876, which was reported in previous study (Yamamoto et al. 2015), and p.(R283Q), which was identified in the patient NS876 as a de novo variant, were overexpressed in NIH3T3 cells. However, the overexpression of *LZTR1* variants did not induce the activation of the ERK- or ELK-mediated transactivation compared with the WT *LZTR1* (Supplemental Fig. 2). Recently, Johnston et al. reported the AR form of NS, suggesting that the identified variants in *LZTR1* could lead to loss-of-function (Johnston et al. 2018). Based on our finding that LZTR1 interacted with the RAF1/SHOC2/PPP1CB complex, we examined the effect of *LZTR1* knockdown on phosphorylation of serine 259 in RAF1 in HEK293 cells, which has an inhibitory role in RAF1 activation. As shown in Fig. 2d, the phospho-RAF1 Ser259 levels were remarkably lower in HEK293 cells transfected with LZTR1 siRNA compared with the control siRNA-transfected cells. These results suggested that LZTR1 was associated with the RAF1/SHOC2/PPP1CB complex and regulated the RAF1 activation.

Discussion

In the current study, we performed targeted NGS sequencing and reexamined the available exome data in 166 patients with certain clinical phenotypes of RASopathies with no mutations in major causal genes. Among the newly identified RASopathy genes reported after 2015, we identified eight *LZTR1* variants in seven patients with NS or suspected Noonan syndrome and a *PPP1CB* variant in a patient with Noonan syndrome. Of the eight *LZTR1* variants, two missense variants, p.(R283Q) and p.(G248R), were concluded to be likely pathogenic. In contrast, the pathogenicity of four identified variants, including c.428A>G, p.(N143S); c.604_605del, p.(M202fs); c.1660G>C, p.(A554P); and c.756_758del, p.(253del), remains inconclusive, because they were identified in a parent without clinical manifestations that are suggestive of NS. Compound heterozygous variants were identified in a patient, who was diagnosed as having AR NS. Functional analysis revealed that LZTR1 was associated with the RAF1/SHOC2/PPP1CB complex and that it could potentially regulate the RAF1 activation. These are the first results demonstrating LZTR1 as a novel regulator of the RAS/MAPK pathway in association with the RAF1/SHOC2/PPP1CB complex.

LZTR1 was identified as a causative gene of RASopathies (Yamamoto et al. 2015); however, whether LZTR1 is a component of the RAS/MAPK signaling pathway remains unknown. By liquid chromatography-tandem mass spectrometry analysis, we identified PPP1CB as a novel interactor of LZTR1. Rodriguez-Viciana et al. showed that PP1C was a highly specific effector of MRAS, which targets SHOC2/

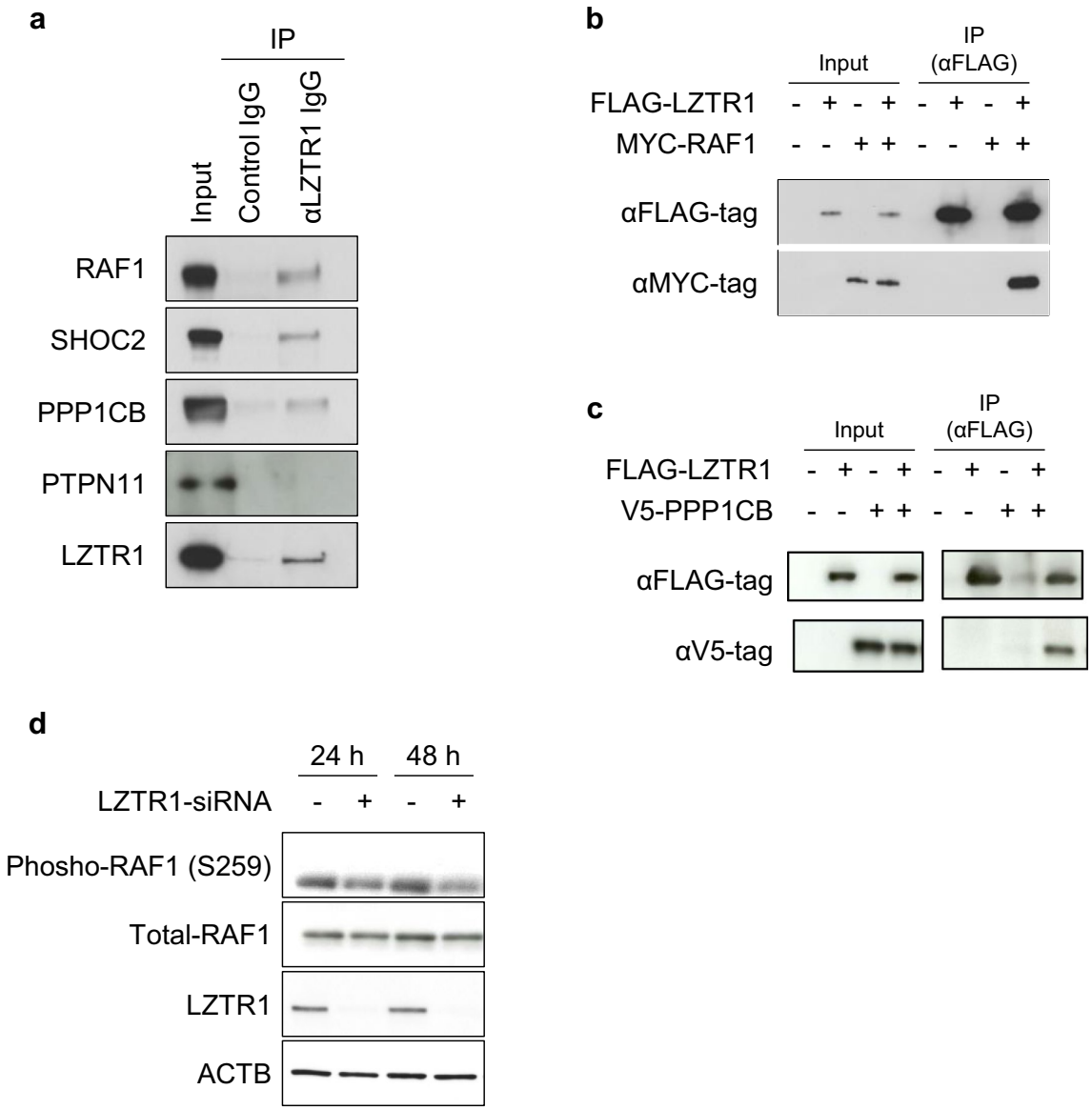

Fig. 2 Effect of LZTR1 on the RAF1/SHOC2/PPP1CB complex. **a** Western blotting of HEK293 cells using antibodies against RAF1, SHOC2, PPP1CB, and PTPN11 following immunoprecipitation by LZTR1. **b, c** Western blotting of HEK293 cells after co-immunoprecipitation using FLAG antibody (**b** LZTR1-FLAG and RAF1-MYC; **c** LZTR1-FLAG and PPP1CB-V5). **d** Western blotting of HEK293 cells using an antibody against phospho-RAF1 (Ser259) in cells transfected with a small interfering RNA against LZTR1 or control. IP, immunoprecipitation

PP1C to stimulate RAF1 activity by dephosphorylating the Ser259 inhibitory site on RAF1 (Rodriguez-Viciana et al. 2006). In fact, we demonstrated the interaction of LZTR1 with RAF1, SHOC2, and PPP1CB (Fig. 2a–c). LZTR1 has six Kelch domains and two BTB domains (Fig. 3a). We examined the amino acid sequence of LZTR1 and recognized that a PP1-binding consensus motif (RVxF), which is present at least one in most interactors of PP1 (Wakula et al. 2003), existed in the Kelch domain at the N-terminus of LZTR1 (Fig. 3b). Furthermore, the cells with *LZTR1* knockdown showed decreased phospho-RAF1-Ser259 levels compared with the control siRNA-transfected cells (Fig. 2d). These results suggest that endogenous LZTR1 could inhibit the activation of RAF1. Taken together, our in vitro findings provide the first evidence that LZTR1 interacts with the RAF1/SHOC2/PPP1CB complex and might regulate RAF1.

We identified eight *LZTR1* variants in seven patients with NS or suspected NS in the current study. Figure 3a summarizes the somatic or germline *LZTR1* mutations reported in NS and schwannomatosis/glioblastoma. In previous studies, almost all *LZTR1* mutations identified in individuals with AD inheritance were located in Kelch 4 and 5 domains

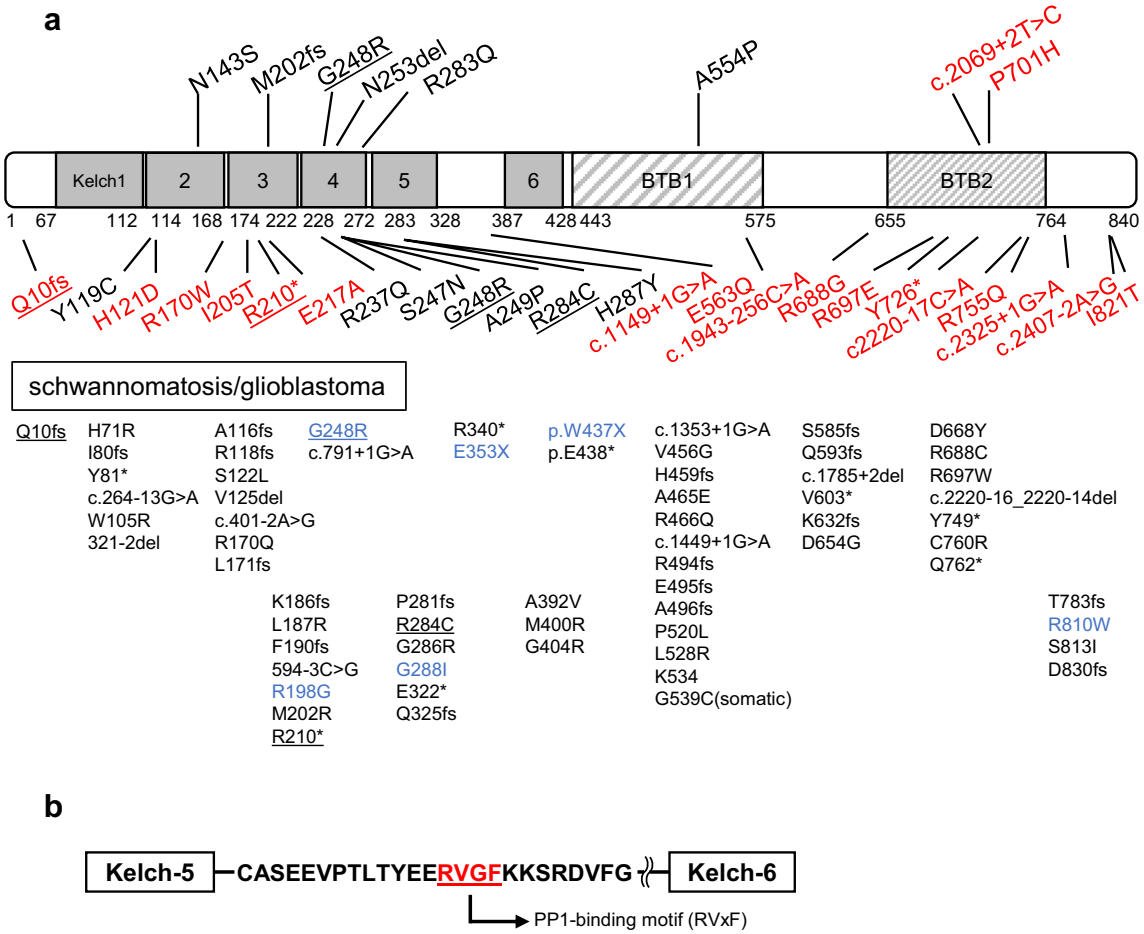

Fig. 3 Schematic structure of *LZTR1* mutations or variants identified to date. **a** LZTR1 has six Kelch domains (gray rectangles) and two BTB domains (striped rectangles) (Nacak et al. 2006). The numbers under the bar denote amino acids. Variants indicated above the bar were identified in the current study. Variants below the bar were reported in previous studies, and lower were detected in schwannomatosis and glioblastoma (blue). Variants indicated underline were detected in multiplicative disease model. Red represents detection in the patients with autosomal recessive disease. **b** Schematic diagram of the partial amino acid sequence of LZTR1. LZTR1 has an RVxF motif, which binds PP1, between the domains Kelch 5 and Kelch 6

(Yamamoto et al. 2015). In contrast, the *LZTR1* mutations identified in individuals with AR inheritance were detected in other domains (Johnston et al. 2018). The variants detected in the current study were located in both the Kelch and BTB domains. We were unable to conclude whether all variants were pathogenic because the three variants were detected in the parents with no clinical manifestations. Only the variants p.(G248R), p.(N253del), and p.(R283Q) were located in Kelch 4 and 5; therefore, it may be considered that the other variants indicate one of the recessive inheritance forms. Somatic or germline mutations of *LZTR1*, which were also reported to cause schwannomatosis (Farschtschi et al. 2016; Hutter et al. 2014; Paganini et al. 2015; Piotrowski et al. 2013; Smith et al. 2015) and glioblastoma (Frattini et al. 2013), do not form noticeable clusters. Most somatic or germline mutations identified in schwannomatosis and glioblastoma are nonsense or frame-shift mutants, suggesting loss-of-function. In our expression experiments, we did not detect any significant changes in the RAS/MAPK signaling pathway in cells overexpressing mutant cDNA harboring c.742G>A, (p.(G248R)) or c.848G>A, (p.(R283Q)), suggesting that variants that cause AD NS might not be gain-of-function mutations (Supplemental Fig. 2). In contrast, given that the cells with *LZTR1* knockdown exhibited decreased phospho-RAF1-Ser259 levels compared with the control siRNA-transfected cells, it is possible that *LZTR1* variants in patients with AR NS might have loss-of-function effects.

As shown in Table 3, we compared the clinical manifestations in seven patients in the current study as well as 34 patients with AD and AR forms of NS that were reported previously (Johnston et al. 2018; Yamamoto et al. 2015). All patients in the current study exhibited cardiac defects. In contrast, 27 of the 34 patients (79.4%) from the previous studies had heart defects. In particular, hypertrophic

cardiomyopathy was more frequent in the current study cohort (71.4%) compared with the earlier study (48.3%). Conversely, the frequency of PS was similar between the current study and two previous studies (28.6% and 24.1%). Furthermore, hyperkeratosis and intellectual disability were more frequently detected in the current study cohort (57.1% vs 7.7%, and 71.4% vs 15.4%). In the previous report of patients with AR inheritance (Johnston et al. 2018), there were four deaths in utero and during childhood because of hydrops fetalis, cardiac defects, or acute myeloblastic leukemia; however, there were no deaths in the current study cohort at the time of the survey. Overall, these findings indicate that the clinical presentation of NS caused by *LZTR1* variants might range from mild to severe symptoms. Because all studies investigated only a small number of patients, further studies are necessary to identify specific clinical manifestations in patients with *LZTR1* variants.

One known variant in *PPP1CB* was detected by the reexamination of the 24 exomes previously sequenced. The patient with the p.P49R variant showed the clinical features of NS. Compared with the previous reports of patients with *PPP1CB* variants (Bertola et al. 2017; Gripp et al. 2016; Ma et al. 2016; Zambrano et al. 2017), our patient did not have hair-associated features; however, he did have other symptoms found in high frequency in those with *PPP1CB* variants, including relative macrocephaly, hypertelorism, cardiac defects, and intellectual disability (Table 4). These results suggest that incorporating *PPP1CB* into the panel may increase the diagnostic rate.

In summary, we identified eight *LZTR1* variants in seven individuals and one *PPP1CB* variant in a patient with NS using an NGS panel. Of the seven patients with *LZTR1* variants, one patient has variants in both alleles, suggesting an AR inheritance of NS. Although there are variants that cannot be concluded as pathogenic, we consider that our data supports the previous report that *LZTR1* is a causative gene of AD or AR NS. Our in vitro analyses demonstrated that LZTR1 interacted with the RAF1/SHOC2/PPP1CB complex and regulated the phosphorylation of Ser259 on RAF1. This is the first study to demonstrate the biochemical evidence

Table 3 Comparison between this study and previous studies on clinical manifestations of patients with *LZTR1* variations

	This study		Previous study[a]	
	n	%	*n*	%
Total	7		34	
Sex (male:female)	4:3		13:21	
Mean age	9.6 years (range 2–16 years)		12.2 years (range 0–69 years)	
Premature birth	2	40.0%	1	12.5%
Short stature	5	71.4%	20	62.5%
Short/webbed neck	5	83.3%	23	71.9%
Pectus deformity	3	42.9%	14	51.9%
Curly hair	2	33.3%	9	33.3%
Hyperkeratosis	4	57.1%	1	7.7%
Naevus	2	28.6%	2	15.4%
Cardiac defects	7	100.0%	27	79.4%
Hypertrophic cardiomyopathy	5	71.4%	14	48.3%
Atrial septal defect	3	42.9%	9	31.0%
Ventricular septal defect	1	14.3%	5	17.2%
Pulmonary stenosis	2	28.6%	7	24.1%
Arrhythmia	1	20.0%	1	3.4%
Other	Patent ductus arteriosus 1 Anomalous origin of coronary artery 1		Left ventricular hypertrophy 1 Mitral valve prolapse 2 Tricuspid valve dysfunction 1 Mitral valve insufficiency 1 Coarctation of aorta 1	
Cryptorchidism	1	25.0%	4	36.4%
Coagulation defects	0	0.0%	2	15.4%
Intellectual disability	5	71.4%	2	15.4%
Miscellaneous			Lacrimal duct obstruction 1 Hemangioma 1 Lymphedema 1 Varicose veins 1	

[a]Yamamoto et al. (2015) and Johnston et al. (2018)

Table 4 Comparison between this study and previous studies on clinical manifestations of patients with *PPP1CB* variations

	This study	Previous study[a]	
		n	%
Total		14	
Sex (male:female)	Male	9:5	
Mean age	16 years	7.3 years (range 4–21 years)	
Relative macrocephaly	+	5	83.3%
Hypertelorism	+	11	78.6%
Downslanting palpebral fissures	−	5	35.7%
Ptosis	+	3	21.4%
Epicanthal folds	+	1	7.1%
Low-set ears	+	8	57.1%
Sparse eyebrows	+	NR	
Bitemporal constriction	+	NR	
Hypoplasia of supraorbital ridges	+	NR	
Short stature	+ (− 2.2 SD)	7	50.0%
Pectus deformity	−	6	42.9%
Curly hair	−	1	7.1%
Cardiac defects	+	12	85.7%
	VSD, PS	ASD 1, VSD 1, PS 2, arrhythmia 1 Left ventricular hypertrophy 1, MS 2 Coarctation of aorta 2 Hypoplastic left aortic arch 1 Patent foramen ovale 2	
Cryptorchidism	+	3	33.3%
Intellectual disability	Mild	14	100.0%
Miscellaneous		Lacrimal duct obstruction 1 Strabismus 1, hearing loss 2 Optic nerve hypoplasia, nystagmus, impaired vision 1, clinodactyly 2 Slow growing hair 8 Unruly hair texture 4	

ASD atrial septal defect, *VSD* ventricular septal defect, *PS* pulmonary stenosis, *MS* mitral stenosis

[a]Gripp et al. (2015), Ma et al. (2016), Zambrano et al. (2017), and Bertola et al. (2017)

for LZTR1 as a component of the RAS/MAPK pathway. Future studies are necessary to elucidate the mechanisms of LZTR1-mediated regulation of the MRAS-RAF1/SHOC2/PPP1CB pathway and the pathogenetic mechanisms of mutant LZTR1 in AD or AR NS.

Materials and methods

Subjects

This study was approved by the Ethics Committee of the Tohoku University School of Medicine. Informed consent was obtained from all subjects involved in the study or their parents.

We included patients who have clinical manifestations related to RASopathies, including relative macrocephaly, short stature, congenital heart defects, hypertrophic cardiomyopathy, distinctive facial appearance, lymphatic abnormalities, and intellectual disability. This study included 142 patients with suspected RASopathies who were not found to have a mutation by Sanger sequence screening that included *PTPN11* (exons 1–15), *SHOC2* (exon 1), *KRAS* (exons 1–5), *RAF1* (exons 7, 14, and 17), *HRAS* (exons 1–5), *BRAF* (exons 6 and 11–16), *MAP2K1* (exons 2 and 3), *MAP2K2* (exons 2 and 3), *SOS1* (exons 1–23), and *RIT1* (exons 1–6).

We previously performed exome sequencing of 24 patients who are diagnosed as having Noonan syndrome and related disorders. We reexamined the excel data if *LZTR1* variants had been identified. Therefore, a total of 166 patients were included in this study.

Targeted NGS

Genomic DNA was extracted from patient blood samples using standard protocols. Sequencing libraries were prepared from genomic DNA using the SureSelect target enrichment

system (Agilent Technologies). Targeted libraries were sequenced using the MiSeq platform according to the manufacturer's instructions (Illumina, San Diego, CA, USA). The analyses were performed according to a previous report (Nishiyama et al. 2017). Paired 151-bp reads were aligned to the reference human genome (UCSC Genome Browser hg19) using the Burrows–Wheeler Alignment tool. Duplicate reads were removed using the Picard software package (http://Picard.sourceforge.net/). Identification of single nucleotide variants and indels calling and depth of coverage analyses were performed with the Genome Analysis Toolkit v3.1. Single nucleotide variants and indels were annotated against the RefSeq and single nucleotide polymorphism databases in the ANNOVAR program (dbSNP142, http://www.ncbi.nlm.nih.gov/projects/SNP/). The PolyPhen2 software (http://genetics.bwh.harvard.edu/pph2/) and SIFT (http://sift.jcvi.org/) were used to assess the functional effects of variants. Novel mutations were extracted according to the variants located in an exon or splice site, excluding synonymous variants, and variants that exhibited a minor allele frequency of less than 1% or were not reported in variant databases in the 1000 Genomes Project (http://browser.1000genomes.org/), the Exome Aggregation Consortium (ExAC, http://exac.broadinstitute.org/), the NHLBI exome sequencing project (ESP6500, http://evs.gs.washington.edu/EVS/), the Human Genome Variation Database (HGVD, http://www.genome.med.kyoto-u.ac.jp/SnpDB/), and the integrative Japanese Genome Variation Database (iJGVD, https://ijgvd.megabank.tohoku.ac.jp/). Detected variants were confirmed through visual examination of the genetic data with the Integrative Genomics Viewer (http://www.broadinstitute.org/igv/). We searched for variants that were listed as RASopathy-causing mutations in the Human Gene Mutation Database (HGMD, http://www.hgmd.org). An average of 99.8% (99.3–100%) and 98.9% (97.9–99.3%) of the overall targeted regions were covered by at least 10 and 30 sequence reads in each sample, respectively. The mean read depth of the all target regions was 214.90. An average of 85.6% (*HRAS*) to 100% (*LZTR1, NRAS, RASA1, RIT2, RRAS*, and *SMARCE1*) of the targeted regions showed at least 10-fold coverage, and 83.85% (*HRAS*) to 100% (*NRAS*) of the targeted regions had at least 30-fold coverage (Supplementary Table 2).

Because *PPP1CB* was reported as a causative gene in NS after the current targeted panel was designed, we searched for *PPP1CB* variants in the previously analyzed data of 24 patients with RASopathies using a similar strategy.

Sanger sequencing

We performed Sanger sequencing to validate the mutations identified by targeted sequencing. Polymerase chain reaction (PCR) of the genomic DNA was performed using custom-designed primers (Supplementary Tables 3 and 4). PCR products were purified using a MultiScreen-PCR plate (Millipore, Billerica, MA, USA) or a QiAquik Gel Extraction Kit (QIAGEN, Hilden, Germany). Sequencing was performed on a 3500xL Genetic Analyzer (Applied Biosystems, Foster City, CA, USA). If splice variants were detected, RNA was extracted from white blood cells using TRIzol® reagent (Invitrogen, Carlsbad, CA, USA), and cDNA was synthesized using High-Capacity cDNA Reverse Transcription Kit (Applied Biosystems) for direct sequencing.

Plasmid preparation

LZTR1 cDNA (OriGene Technologies, Rockville, MD, USA) was amplified by PCR, with the addition of a FLAG tag at the C-terminus. FLAG-tagged *LZTR1* variants (c.742G>A, p.(G248R) and c.848G>A, p.(R283Q)) were generated using a wild-type (WT) *LZTR1* cDNA with the QuikChange Site-Directed Mutagenesis Kit (Agilent Technology) according to the manufacturer's instructions. Mutagenic primers were designed using the web-based QuikChange Primer Design Program. The WT and mutated cDNAs were subcloned into the pCAGGS vector (Niwa et al. 1991). MYC-tagged *RAF1* cDNA was created previously (Kobayashi et al. 2010). *PPP1CB* cDNA was amplified by PCR from human cDNA and constructed using the pENTR-SD-D-TOPO Gateway cloning system (Invitrogen) following standard protocols, and pENTR-*PPP1CB* was subcloned into the pcDNA3.2/V5-DEST Mammalian Expression Vector. All mutated plasmids were sequenced to verify the mutations (Supplementary Table 5).

Western blotting

We performed western blotting to examine the effect of *LZTR1* variations identified in the current study on the downstream signaling activity of RAS. NIH3T3 cells were purchased from the American Type Culture Collection (ATCC, Rockville, MD, USA). Cells were cultured in Dulbecco's modified Eagle medium supplemented with 10% NCS, 100 U/ml penicillin, and 100 µg/ml streptomycin in a CO_2 incubator with 5% CO_2 at 37 °C. NIH3T3 cells were seeded at a concentration of 3×10^5 cells in 6-cm dishes and incubated at 37 °C. After 16 h, the cells were transfected with 4.0 µg pCAGGS plasmids encoding WT *LZTR1, LZTR1* variants, or mouse *Braf* V637E (positive control corresponding to the *BRAF* V600E mutation in humans) using 8 µl PLUS reagent and 12 µl Lipofectamine reagent (Invitrogen). The medium was replaced with fresh complete medium three hours after transfection, and the cells were incubated for another 45 h. Next, the cells were scraped and washed twice with phosphate-buffered saline (PBS) using centrifugation. The pelleted cells were lysed in 100 µl lysis

buffer (10 mM Tris–HCl pH 7.5 and 1% SDS) and boiled for 5 min. The DNA was sheared with a syringe. The lysates were centrifuged at 15,000 rpm for 10 min, and protein concentrations were determined by the Bradford assay (Bio-Rad, Hercules, CA, USA). Fifteen µg protein per sample was separated by 5–20% gradient SDS–polyacrylamide gel electrophoresis (ATTO, Tokyo, Japan) and transferred to nitrocellulose membranes. The following antibodies were used: LZTR1 (sc-390166), PTPN11 (sc-7384) from Santa Cruz Biotechnology (Dallas, TX, USA); FLAG (F1804) from Sigma-Aldrich (St. Louis, MO, USA); MYC-Tag (2278), SHOC2 (53600), phospho-c-RAF (Ser259; 9421), ERK1/2 (9102), phospho-ERK1/2 (9101), p38 (8690), phospho-p38 (4511), AKT (9272), and phospho-AKT (S473; 9271, T308, 2965) from Cell Signaling (Danvers, MA, USA); RAF1 (610152) from BD Biosciences (Franklin Lakes, NJ, USA); and PPP1CB (ab53315) from Abcam (Cambridge, UK). All membranes were visualized using the Western Lightning ECL-Plus kit (Perkin-Elmer, Waltham, MA, USA).

Luciferase assay

The following plasmids were purchased from Agilent Technologies: pFR-luc, pFA2-Elk1, pFA2-c-Jun, pFA2-CHOP, pFC-MEK1, pFC-MEKK, pFC-MEK3, and pFC2-dbd. PRL-null was purchased from Promega (Madison, WI, USA). NIH3T3 cells were maintained as described above. We assessed the activation of the MAPK signaling pathway in NIH3T3 cells using the PathDetect Trans-Reporting system (Agilent Technologies). We performed transfections and the assays as previously reported (Yaoita et al. 2016).

Statistical analyses were performed using Excel (Microsoft, Redmond, WA, USA). The significance of differences between the control and treated groups was determined by Student's *t* test. $P < 0.05$ was considered statistically significant for analyses performed.

Immunoprecipitation

HEK293 cells were purchased from the ATCC and maintained in 15-cm dishes with Dulbecco's modified Eagle medium supplemented with 10% fetal bovine serum, 100 U/ml penicillin and 100 µg/ml streptomycin in a CO_2 incubator with 5% CO_2 at 37 °C. Cells were collected and lysed with a HEPES-based buffer [25 mM HEPES pH 7.5, 300 mM NaCl, 0.2% NP40, and 1:100 protease inhibitor cocktail (Sigma-Aldrich)]. The sonicated and filtered cell lysates were centrifuged to remove unlysed cells, and the supernatants were collected and incubated with benzonase (Merck, Darmstadt, Germany), Dynabeads protein G (Thermo Fisher Scientific, Waltham, MA, USA), and a control anti-mouse IgG or an anti-LZTR1 antibody (sc-390731; Santa Cruz Biotechnology) overnight at 4 °C. Next, the beads were washed three times with a buffer containing 50 mM HEPES pH 7.5, 150 mM NaCl, and 0.1% NP40 and one time with PBS. The immune complexes were eluted by a buffer containing 1.2 M NaCl and analyzed by western blotting as described above.

Co-immunoprecipitation

HEK293 cells were seeded at a density of 6×10^6 cells in 15-cm dishes. Twenty hours later, the cells were transfected with expression plasmids encoding LZTR1-FLAG and RAF1-MYC or LZTR1-FLAG and PPP1CB-V5. Forty-eight hours later, the cells were lysed using a buffer containing 50 mM Tris HCl pH 7.4, 150 mM NaCl, 1 mM EDTA, and 1% Triton X-100. The sonicated cell lysates were rotated with an affinity gel containing an anti-FLAG M2 antibody (Sigma-Aldrich), MYC-tag Sepharose beads (Cell Signaling Technology), or an anti-V5-tag antibody (MBL, Nagoya, Japan) overnight at 4 °C. After washing the gel or the beads three times in Tris-buffered saline buffer and one time in PBS, the immune complexes were eluted with 0.1 M glycine buffer (pH 2.0) and analyzed by western blotting as described above.

Small interfering RNA transfection

ON-TARGETplus Non-Targeting Pool (control small interfering RNA [siRNA], #D-001810-10) or ON-TARGETplus SMART Pool-human LZTR1 (LZTR1 siRNA, #L-012318) were purchased from GE Healthcare Dharmacon (Lafayette, CO, USA). HEK293 cells were transfected with 10 nM control or LZTR1 siRNA using Lipofectamine RNAiMAX (Thermo Fisher Scientific). Twenty-four hours later, the cells were washed to remove the medium and replaced with fresh medium containing serum.

Acknowledgements The authors thank the patients, their family members, and the doctors who participated in this study. We are grateful to Jun-ichi Miyazaki of Osaka University for supplying the pCAGGS expression vector. We thank Daiju Oba, Ayumi Nishiyama, Shingo Takahara, Aya Shibui-Inoue, Yu Katata and Koki Nagai who contributed to the routine diagnostic work, and Yoko Tateda, Kumi Kato, and Riyo Takahashi for their technical assistance.

Funding This study was supported in part by the Grants-in-Aid by the Practical Research Project for Rare/Intractable Diseases from the Japan Agency for Medical Research and Development, AMED to Y.A. (18ek0109241h0002), and the Japan Society for the Promotion of Science (JSPS) KAKENHI Grant Numbers 17H04223 to Y.A. and 18K15657 to T.A.

Compliance with ethical standards

Conflict of interest The authors declare that they have no conflict of interest.

References

Aoki Y, Niihori T, Narumi Y, Kure S, Matsubara Y (2008) The RAS/MAPK syndromes: novel roles of the RAS pathway in human genetic disorders. Hum Mutat 29:992–1006. https://doi.org/10.1002/humu.20748

Aoki Y, Niihori T, Banjo T, Okamoto N, Mizuno S, Kurosawa K, Ogata T, Takada F, Yano M, Ando T, Hoshika T, Barnett C, Ohashi H, Kawame H, Hasegawa T, Okutani T, Nagashima T, Hasegawa S, Funayama R, Nagashima T, Nakayama K, Inoue S, Watanabe Y, Ogura T, Matsubara Y (2013) Gain-of-function mutations in RIT1 cause Noonan syndrome, a RAS/MAPK pathway syndrome. Am J Hum Genet 93:173–180. https://doi.org/10.1016/j.ajhg.2013.05.021

Bertola D, Yamamoto G, Buscarilli M, Jorge A, Passos-Bueno MR, Kim C (2017) The recurrent PPP1CB mutation p.Pro49Arg in an additional Noonan-like syndrome individual: Broadening the clinical phenotype. Am J Med Genet A 173:824–828. https://doi.org/10.1002/ajmg.a.38070

Chen PC, Yin J, Yu HW, Yuan T, Fernandez M, Yung CK, Trinh QM, Peltekova VD, Reid JG, Tworog-Dube E, Morgan MB, Muzny DM, Stein L, McPherson JD, Roberts AE, Gibbs RA, Neel BG, Kucherlapati R (2014) Next-generation sequencing identifies rare variants associated with Noonan syndrome. Proc Natl Acad Sci USA 111:11473–11478. https://doi.org/10.1073/pnas.1324128111

Farschtschi S, Mautner VF, Pham M, Nguyen R, Kehrer-Sawatzki H, Hutter S, Friedrich RE, Schulz A, Morrison H, Jones DT, Bendszus M, Baumer P (2016) Multifocal nerve lesions and LZTR1 germline mutations in segmental schwannomatosis. Ann Neurol 80:625–628. https://doi.org/10.1002/ana.24753

Frattini V, Trifonov V, Chan JM, Castano A, Lia M, Abate F, Keir ST, Ji AX, Zoppoli P, Niola F, Danussi C, Dolgalev I, Porrati P, Pellegatta S, Heguy A, Gupta G, Pisapia DJ, Canoll P, Bruce JN, McLendon RE, Yan H, Aldape K, Finocchiaro G, Mikkelsen T, Prive GG, Bigner DD, Lasorella A, Rabadan R, Iavarone A (2013) The integrated landscape of driver genomic alterations in glioblastoma. Nat Genet 45:1141–1149. https://doi.org/10.1038/ng.2734

Gripp KW, Aldinger KA, Bennett JT, Baker L, Tusi J, Powell-Hamilton N, Stabley D, Sol-Church K, Timms AE, Dobyns WB (2016) A novel rasopathy caused by recurrent de novo missense mutations in PPP1CB closely resembles Noonan syndrome with loose anagen hair. Am J Med Genet A 170:2237–2247. https://doi.org/10.1002/ajmg.a.37781

Higgins EM, Bos JM, Mason-Suares H, Tester DJ, Ackerman JP, MacRae CA, Sol-Church K, Gripp KW, Urrutia R, Ackerman MJ (2017) Elucidation of MRAS-mediated Noonan syndrome with cardiac hypertrophy. JCI Insight 2:e91225. https://doi.org/10.1172/jci.insight.91225

Hutter S, Piro RM, Reuss DE, Hovestadt V, Sahm F, Farschtschi S, Kehrer-Sawatzki H, Wolf S, Lichter P, von Deimling A, Schuhmann MU, Pfister SM, Jones DTW, Mautner VF (2014) Whole exome sequencing reveals that the majority of schwannomatosis cases remain unexplained after excluding SMARCB1 and LZTR1 germline variants. Acta Neuropathol 128:449–452. https://doi.org/10.1007/s00401-014-1311-1

Johnston JJ, van der Smagt JJ, Rosenfeld JA, Pagnamenta AT, Alswaid A, Baker EH, Blair E, Borck G, Brinkmann J, Craigen W, Dung VC, Emrick L, Everman DB, van Gassen KL, Gulsuner S, Harr MH, Jain M, Kuechler A, Leppig KA, McDonald-McGinn DM, Can NTB, Peleg A, Roeder ER, Rogers RC, Sagi-Dain L, Sapp JC, Schaffer AA, Schanze D, Stewart H, Taylor JC, Verbeek NE, Walkiewicz MA, Zackai EH, Zweier C, Zenker M, Lee B, Biesecker LG (2018) Autosomal recessive Noonan syndrome associated with biallelic LZTR1 variants. Genet Med. https://doi.org/10.1038/gim.2017.249

Kobayashi T, Aoki Y, Niihori T, Cave H, Verloes A, Okamoto N, Kawame H, Fujiwara I, Takada F, Ohata T, Sakazume S, Ando T, Nakagawa N, Lapunzina P, Meneses AG, Gillessen-Kaesbach G, Wieczorek D, Kurosawa K, Mizuno S, Ohashi H, David A, Philip N, Guliyeva A, Narumi Y, Kure S, Tsuchiya S, Matsubara Y (2010) Molecular and clinical analysis of RAF1 in Noonan syndrome and related disorders: dephosphorylation of serine 259 as the essential mechanism for mutant activation. Hum Mutat 31:284–294. https://doi.org/10.1002/humu.21187

Lu A, Pfeffer SR (2014) A CULLINary ride across the secretory pathway: more than just secretion. Trends Cell Biol 24:389–399. https://doi.org/10.1016/j.tcb.2014.02.001

Ma L, Bayram Y, McLaughlin HM, Cho MT, Krokosky A, Turner CE, Lindstrom K, Bupp CP, Mayberry K, Mu W, Bodurtha J, Weinstein V, Zadeh N, Alcaraz W, Powis Z, Shao Y, Scott DA, Lewis AM, White JJ, Jhangiani SN, Gulec EY, Lalani SR, Lupski JR, Retterer K, Schnur RE, Wentzensen IM, Bale S, Chung WK (2016) De novo missense variants in PPP1CB are associated with intellectual disability and congenital heart disease. Hum Genet 135:1399–1409. https://doi.org/10.1007/s00439-016-1731-1

Nacak TG, Leptien K, Fellner D, Augustin HG, Kroll J (2006) The BTB-kelch protein LZTR-1 is a novel Golgi protein that is degraded upon induction of apoptosis. J Biol Chem 281:5065–5071. https://doi.org/10.1074/jbc.M509073200

Nava C, Hanna N, Michot C, Pereira S, Pouvreau N, Niihori T, Aoki Y, Matsubara Y, Arveiler B, Lacombe D, Pasmant E, Parfait B, Baumann C, Heron D, Sigaudy S, Toutain A, Rio M, Goldenberg A, Leheup B, Verloes A, Cave H (2007) Cardio-facio-cutaneous and Noonan syndromes due to mutations in the RAS/MAPK signalling pathway: genotype-phenotype relationships and overlap with Costello syndrome. J Med Genet 44:763–771. https://doi.org/10.1136/jmg.2007.050450

Nishiyama A, Niihori T, Warita H, Izumi R, Akiyama T, Kato M, Suzuki N, Aoki Y, Aoki M (2017) Comprehensive targeted next-generation sequencing in Japanese familial amyotrophic lateral sclerosis. Neurobiol Aging 53:194.e1–194.e194. https://doi.org/10.1016/j.neurobiolaging.2017.01.004 e8.

Niwa H, Yamamura K, Miyazaki J (1991) Efficient selection for high-expression transfectants with a novel eukaryotic vector. Gene 108:193–199

Paganini I, Chang VY, Capone GL, Vitte J, Benelli M, Barbetti L, Sestini R, Trevisson E, Hulsebos TJ, Giovannini M, Nelson SF, Papi L (2015) Expanding the mutational spectrum of LZTR1 in schwannomatosis. Eur J Hum Genet 23:963–968. https://doi.org/10.1038/ejhg.2014.220

Piotrowski A, Xie J, Liu YF, Poplawski AB, Gomes AR, Madanecki P, Fu C, Crowley MR, Crossman DK, Armstrong L, Babovic-Vuksanovic D, Bergner A, Blakeley JO, Blumenthal AL, Daniels MS, Feit H, Gardner K, Hurst S, Kobelka C, Lee C, Nagy R, Rauen KA, Slopis JM, Suwannarat P, Westman JA, Zanko A, Korf BR, Messiaen LM (2013) Germline loss-of-function mutations in LZTR1 predispose to an inherited disorder of multiple schwannomas. Nat Genet 46:182–187. https://doi.org/10.1038/ng.2855

Rodriguez-Viciana P, Oses-Prieto J, Burlingame A, Fried M, McCormick F (2006) A phosphatase holoenzyme comprised of Shoc2/Sur8 and the catalytic subunit of PP1 functions as an M-Ras effector to modulate Raf activity. Mol Cell 22:217–230. https://doi.org/10.1016/j.molcel.2006.03.027

Smith MJ, Isidor B, Beetz C, Williams SG, Bhaskar SS, Richer W, O'Sullivan J, Anderson B, Daly SB, Urquhart JE, Fryer A, Rustad CF, Mills SJ, Samii A, du Plessis D, Halliday D, Barbarot S, Bourdeaut F, Newman WG, Evans DG (2015) Mutations in LZTR1 add to the complex heterogeneity of schwannomatosis. Neurology 84:141–147. https://doi.org/10.1212/WNL.0000000000001129

Stogios PJ, Prive GG (2004) The BACK domain in BTB-kelch proteins. Trends Biochem Sci 29:634–637. https://doi.org/10.1016/j.tibs.2004.10.003

Villani A, Greer MC, Kalish JM, Nakagawara A, Nathanson KL, Pajtler KW, Pfister SM, Walsh MF, Wasserman JD, Zelley K, Kratz CP (2017) Recommendations for cancer surveillance in individuals with RASopathies and other rare genetic conditions with increased cancer risk. Clin Cancer Res 23:e83–e90. https://doi.org/10.1158/1078-0432.CCR-17-0631

Vissers LE, Bonetti M, Paardekooper Overman J, Nillesen WM, Frints SG, de Ligt J, Zampino G, Justino A, Machado JC, Schepens M, Brunner HG, Veltman JA, Scheffer H, Gros P, Costa JL, Tartaglia M, van der Burgt I, Yntema HG, den Hertog J (2015) Heterozygous germline mutations in A2ML1 are associated with a disorder clinically related to Noonan syndrome. Eur J Hum Genet 23:317–324. https://doi.org/10.1038/ejhg.2014.115

Wakula P, Beullens M, Ceulemans H, Stalmans W, Bollen M (2003) Degeneracy and function of the ubiquitous RVXF motif that mediates binding to protein phosphatase-1. J Biol Chem 278:18817–18823

Yamamoto GL, Aguena M, Gos M, Hung C, Pilch J, Fahiminiya S, Abramowicz A, Cristian I, Buscarilli M, Naslavsky MS, Malaquias AC, Zatz M, Bodamer O, Majewski J, Jorge AA, Pereira AC, Kim CA, Passos-Bueno MR, Bertola DR (2015) Rare variants in SOS2 and LZTR1 are associated with Noonan syndrome. J Med Genet 52:413–421. https://doi.org/10.1136/jmedgenet-2015-103018

Yaoita M, Niihori T, Mizuno S, Okamoto N, Hayashi S, Watanabe A, Yokozawa M, Suzumura H, Nakahara A, Nakano Y, Hokosaki T, Ohmori A, Sawada H, Migita O, Mima A, Lapunzina P, Santos-Simarro F, Garcia-Minaur S, Ogata T, Kawame H, Kurosawa K, Ohashi H, Inoue SI, Matsubara Y, Kure S, Aoki Y (2016) Spectrum of mutations and genotype–phenotype analysis in Noonan syndrome patients with RIT1 mutations. Hum Genet 135:209–222. https://doi.org/10.1007/s00439-015-1627-5

Young LC, Hartig N, Munoz-Alegre M, Oses-Prieto JA, Durdu S, Bender S, Vijayakumar V, Vietri Rudan M, Gewinner C, Henderson S, Jathoul AP, Ghatrora R, Lythgoe MF, Burlingame AL, Rodriguez-Viciana P (2013) An MRAS, SHOC2, and SCRIB complex coordinates ERK pathway activation with polarity and tumorigenic growth. Mol Cell 52:679–692. https://doi.org/10.1016/j.molcel.2013.10.004

Zambrano RM, Marble M, Chalew SA, Lilje C, Vargas A, Lacassie Y (2017) Further evidence that variants in PPP1CB cause a rasopathy similar to Noonan syndrome with loose anagen hair. Am J Med Genet A 173:565–567. https://doi.org/10.1002/ajmg.a.38056

Zhang Y, Dong C (2007) Regulatory mechanisms of mitogen-activated kinase signaling. Cell Mol Life Sci 64:2771–2789. https://doi.org/10.1007/s00018-007-7012-3